DF/ab

CERN/MPS/SR 69-11
10th October, 1969

A RESONANT CHARGING PULSED POWER SUPPLY FOR KICKER MAGNET PULSE FORMING NETWORKS

by

D. C. Fiander and P. D. Pearce

Summary

The report describes a resonant power supply which would be suitable for fast recharging of pulse forming networks of a kicker magnet system. The power supply differs from those described in earlier reports in having a high voltage diode in series with the output. The principles are discussed and formulae given which permit the power supply performance to be predicted. Operating experience with a prototype unit is described and oscillograms of single shot and multi-shot operation included.

PS/7457

LIST OF CONTENTS

1. Introduction

Reports [1,2] have already been published which demonstrate the feasability of using a resonant charging pulsed power supply for the pulse forming networks of kicker systems. The present report is concerned with further developments to the previous circuits in order to provide improved flexibility, faster recovery and simpler circuitry.

The resonant power supply operates on the principle of charge transfer from a low voltage primary electrolytic capacitor to a high voltage load capacitor, the transfer being effected through the magnetic circuit of a high ratio transformer. The time of transfer is determined by the resonant frequency of the primary and load capacitors together with the leakage inductance of the transformer.

Three basic changes have been introduced to the circuitry described by previous workers:

1. A three winding transformer has been chosen
2. An uninterrupted D.C. source has been applied to the third winding to provide the transformer core bias
3. A high voltage diode has been inserted between the transformer HT terminal and the load capacitance.

These changes were introduced primarily to improve the core recovery time in order to use the power supply for high repetition rates. However, they also bring with them certain other advantages, discussed in detail in the report, which could justify their use in power supplies intended for low repetition rates in which core recovery time is not of prime importance.

2. List of symbols

C_0	=	Primary capacitor
C_L	=	Load capacitor
C_X	=	Filter capacitor
C_S	=	Transformer secondary stray capacitance
D_1	=	HT diode in series with transformer bushing
D_2	=	Charging circuit diode
SCR1	=	SCR controlling primary capacitor C_0
L_P	=	Primary leakage inductance
L_S	=	Secondary leakage inductance
L_M	=	Magnetising inductance
R_P	=	Primary circuit resistance
R_S	=	Secondary circuit resistance
R_X	=	Filter resistor
R_L	=	Load resistor
R_B	=	Bias circuit resistor
R_C	=	Equivalent core resistance
R_A	=	Charging resistor
G_1	=	D.C. source for charging C_0
G_2	=	D.C. source for bias current I_B
V_0	=	Primary capacitor voltage
V_T	=	Transformer secondary terminal voltage
V_L	=	Load voltage
V_B	=	Driving voltage of G_2
I_P	=	Primary current
I_S	=	Secondary current
I_L	=	Load current
I_M	=	Magnetising current
I_{MO}	=	Magnetising current on completion of charge transfer
ΔI	=	Change in magnetising current associated with total flux charge ΔB of transformer core during charge transfer.

3. Circuitry

The physical circuit of the power supply is shown in Fig. 1. The generator G_1 is a comparatively weak source which suffices to recharge C_0 via R_A between shots but otherwise plays no part in the operation. The primary capacitor C_0 is controlled by SCR1 and is connected directly to the primary winding of the 3 winding transformer. The secondary (HT) winding has one end commoned to the tertiary and grounded. The secondary HT terminal is connected to diode D_1 which in turn is connected to a filter C_X, R_X, intended for transformer secondary winding protection, and then to the load capacitor C_L. External circuitry permits the rapid discharge of C_L via a triggered spark gap (TSG) into a load resistor R_L. The tertiary circu t consists of a D.C. source V_B driving through a series resistor R_B thus circulating D.C. current in the tertiary winding.

The full equivalent circuit for this arrangement is shown in Fig. 2. In particular is to be noted the existance of C_S', the referred value of the transformer secondary winding and bushing capacitance with respect to ground. This capacitance is an essential element in the core recovery process as will be shown in section 4. In fig. 2 all elements have been transferred to the primary side. This procedure will be followed throughout the report and all equations will be based on primary referred values.

4. Theory of operation

The operation of a resonant charging pulsed power supply can be divided into a number of distinct stages. These stages are considered in detail in the order in which they occur, namely:

Stage 1 - the charge transfer period when energy is taken from the primary capacitor C_0 and deposited in the load capacitor C_L

Stage 2 - the disconnection of the primary capacitor C_0 from the system

Stage 3 - the core recovery period

Stage 4 - a modification of the core recovery consequent upon the discharge of the load capacitor C_L during stage 3.

4.1 Stage 1

The starting point of this stage is with the primary capacitor C_0 charged to a voltage V_0 and the transformer core premagnetised to a known flux density by the bias current I_B flowing in the tertiary. The load and filter capacitors C_L and C_X are assumed to be discharged.

The equivalent circuit of Fig. 2 may be reduced to that of Fig. 3 for the charge transfer period without the introduction of significant errors. The performance of this circuit during charge transfer has been fully described elsewhere[2] and will not be developed here. The performance can be summarised by the equations for the load voltage V_L, current I_L, and the resonant frequency $p/2\pi$.

$$V_L' = V_0 \frac{\alpha}{1+\alpha}\left[1 - e^{-\frac{R_\sigma t}{2L_\sigma}}\left(\cos pt + \frac{R_\sigma}{2L_\sigma p}\sin pt\right)\right]$$

$$p^2 = \frac{1+\alpha}{C_0 L_\sigma} - \frac{R_\sigma^2}{4L_\sigma^2}$$

$$I_L' = V_0 \frac{C_0}{1+\alpha} \cdot e^{-\frac{R_\sigma t}{2L_\sigma}}\left(p + \frac{R_\sigma^2}{4pL_\sigma^2}\right)\sin pt.$$

The charge transfer period is completed when I_L passes through zero as the diode D_1 prevents reverse conduction. Charge transfer is thus accomplished in a time $T_1 = \frac{\pi}{p}$. At the end of charge transfer the core induction will have changed because of the unidirectional voltage applied to the transformer. The voltage time integral referred to the primary is given by $V_L' \Phi T_1$ where Φ is a constant determined by the circuit components. It has already been shown (2) that this constant can be evaluated as follows

$$\Phi = \frac{1}{\rho} \frac{\sqrt{4Q^2-1}}{2\pi Q^2}\left(1 - \frac{1+\alpha}{\alpha} \cdot \frac{R_2'}{R_1+R_2'}\right)$$

where R_1 and R_2 are the values of R_σ associated with the primary and secondary sides of the transformer respectively

Q is the quality factor given by $\frac{1}{R_\sigma}\sqrt{(1+\alpha)\frac{L_\sigma}{C_0}}$

$$\rho = 1 + e^{-\frac{\pi}{\sqrt{4Q^2-1}}}$$

The completion of charge transfer is characterised by the abrupt cut-off of load current I_L by diode D_1 and the existence of a magnetising current I_{MO} flowing in the magnetising reactance L_M corresponding to the core induction at the end of charge transfer. This assumes that the current I_{MO} is positive, i.e. that the core has been driven from a state of reverse induction to forward induction by the voltage time integral during charge transfer. This would normally be the case in an efficiently designed and operated system. However, should I_{MO} be negative then the completion of charge transfer is not determined by D_1 but by SCR1 which disconnects the primary capacitor C_0 when the resultant of $+ I_L$ and $- I_{MO}$ is zero. To all practical purposes this would not alter the charge transfer time T_1. The system can clearly work satisfactorily, if inefficiently, in this mode. It is therefore not interesting to consider it further but rather to concentrate on the case where I_{MO} is positive.

4.2 Stage 2

This is the stage which results in the disconnection of the primary capacitor C_0 from the system. Initially a positive current I_{MO} is assumed flowing in L_M, and the secondary stray capacitance of the transformer C_S is charged to V_L. The capacitor C_0 will be disconnected at the first current zero in SCR1. The simplified equivalent circuit for this stage is shown in Fig. 4 on the assumption that the duration of the stage is very short and that the core induction remains constant throughout. It is seen that a resonance occurs between C_S' and L_σ, which due to the low value of C_S normally found in HT transformers gives rise to a frequency considerably higher than in stage 1, i.e. leading to rapid disconnection of C_0 as soon as the current reaches $- I_{MO}$. The initial value of voltage on C_0 is no longer V_0 but xV_0, the final value at the end of charge transfer which may be obtained from the equations of stage 1.

The build-up of current is given by

$$i = \left(xV_0 - V_L{}'\right) \sqrt{\frac{C_S{}'}{L_\sigma}} \sqrt{\frac{\beta}{1+\beta}} \sin pt$$

where $\beta = \frac{C_0}{C_S{}'}$

$$p^2 = \frac{1+\beta}{\beta} \cdot \frac{1}{L_\sigma C_S{}'}$$

As $V_L{}'$ is always greater than xV_0, the current always builds up in the negative sense and commutates the positive magnetising current I_{MO}. When SCR1 becomes open circuit, the core magnetising current I_{MO} which was previously drawn from C_0 is diverted to the secondary and tertiary windings which is the beginning of the next stage, the core recovery.

4.3 Stage 3

This satge is concerned with the recovery of the transformer core from its induction at the end of charge transfer (and also stage 2) back to that prevailing before the start of stage 1. The full equivalent circuit may be simplified to that of Fig. 5. At the start of this stage the current in L_M is + I_{MO} and the voltage on C_S is assumed to be V_L (this assumption is based on a negligible run-down of C_S during stage 2). A resonance occurs between L_M and C_S which is damped by the tertiary resistance R_B and the core loss resistance R_C. The transformer terminal voltage V_T may be determined from

$$V_T' = e^{-\frac{t}{2RC_S'}} \left\{ V_L' \cos pt - \left(\frac{V_L'}{2pRC_S'} + \frac{\Delta I}{pC_S'} \right) \sin pt \right\}$$

where $R = \frac{R_B'' R_C}{R_B'' + R_C}$

$$p^2 = \frac{1}{L_M C_S'} - \frac{1}{4R^2 C_S'^2}$$

ΔI is the total change of magnetising current corresponding to the full flux swing ΔB occurring during charge transfer.

The magnetising current in L_M is given by

$$I_M = e^{-\frac{t}{2RC_S'}} \left\{ \Delta I \cos pt + \frac{\sin pt}{p} \left(\frac{V_L'}{4R^2 C_S'} + \frac{\Delta I}{2RC_S'} + V_L' C_S' p^2 \right) \right\} - \frac{V_B''}{R_B''}$$

It is to be noted that at t_∞ the magnetising current is equal to the referred tertiary d.c. current.

The resonance arising during this stage is such as to cause the transformer voltage V_T to become negative and hence to force the recovery of the transformer core to its initial state of induction. Typical waveforms of the transformer secondary voltage V_T and magnetising current I_M are shown in Fig. 7. V_T increases to its maximum value V_L during the charge transfer period (stage 1). It then remains approximately constant during AB, the commutation period of SCR1 (stage 2). In stage 3 the load voltage V_L remains constant and V_T oscillates according to the above equation. Recovery of the core is complete when the resultant area under the V_T curve is zero and when I_M is equal to $- V_B''/R_B''$. It should be noted that the induction of the core becomes more positive for some time after the end of charge transfer. Maximum positive flux is reached at point C of Fig. 7 which corresponds to $\hat{I}_M$ - consequently the design of a given system must take this into account. Point D corresponds to minimum induction in the core and in fact to an induction more negative than the initial biased starting point. This also has to be taken into account in order not to choose too large a bias leading to negative saturation at D. The total positive transformer flux swing is determined by the area OABC. It is clearly desirable to keep this to a minimum in order to reduce the transformer kVA rating. OAE is due to the charge transfer, ABEF is due to SCR commutation and is negligible in practice, and BFC is due to the recovery resonance. This latter will be a minimum if the resonant frequency of stage 3 is a maximum, i.e. if C_S is low and L_M is low. For efficient charge transfer L_M must not be low, so the only method of ensuring a minimum area for BFC is to keep C_S low.

The V_T underswing is principally determined by ΔI, the total change of magnetising current corresponding to the ΔB during charge transfer, and the damping resistor R_B of the tertiary. Changing R_B from a high value to a low value increases the damping of stage 3, finally changing stage 3 from oscillatory to overdamped.

Unlike the systems already reported on, the transformer induction of the present system does not depend on the duration of the flat top voltage V_L. V_L may be retained indefinitely without altering the core recovery time. However, operation of the triggered spark gap TSG during period BC does shorten marginally the core recovery as V_T is forced to zero and some of the area BFC is lost.

This may not be a desirable method of operation as it exposes the transformer secondary winding to some surge voltage, reduced in severity by C_X and R_X. A more desirable zone for operation of TSG is in CD as here the surge is held by D_1. However, the equations of stage 3 no longer apply on reaching point D when V_T begins to go positive again. This leads to the situation described below in stage 4.

4.4 Stage 4

This stage is defined from point D onwards when the load capacitor has been discharged prior to D. The positive going voltage V_T sees not only C_S but also C_X and C_L through diode D_1. The resonance is changed to that between L_M and $C_X + C_L$. The approximate equivalent circuit is changed to that of Fig. 6. C_S may be ignored in relation to $C_X + C_L$ for the period when $V_T > V_L$. The equations of stage 3 apply subject to the substitution of $C_X' + C_L'$ for C_S'. In practice the effect is to reduce the frequency of resonance by an order of magnitude and hence to reduce the positive going excursion of V_T because of the damping.

5. Advantages and disadvantages of the present system

In relation to the resonant power supplies already proposed separately by Messrs. Brückner and Cupérus, the present system is considered to offer the following advantages:

a) improved flexibility in that the duration of the load voltage flat top does not influence the performance of the power supply

b) efficient use of the transformer core because core recovery begins automatically on completion of charge transfer

c) minimum complication in the bias circuitry and the elimination of all bias switching

d) faster core recovery which may be controlled by the damping resistor of the tertiary winding

e) elimination of all reverse voltage from the load, with consequent easing of the high voltage specification for pulse forming network and switchgear.

The following disadvantages must also be considered:

a) the need to use a 3 winding transformer

b) the power loss in the tertiary damping resistor (typically 40 - 200 watts in a 20 kVA installation)

c) the additional cost of a high voltage diode able to withhold about 1.5 V_L (typically 2000 SFr.)

d) the need to specify carefully not only the transformer leakage reactance but also its secondary stray capacitance.

e) All resonant power supplies demand a well defined initial load voltage (normally zero) prior to charge transfer if good stability of the final load voltage V_L is to be obtained. In the case of resonant power supplies in which the load is connected directly to the transformer secondary V_L must sooner or later collapse to zero because of transformer core saturation. Thus, if the power supply repetition rate is sufficiently slow no problem would arise should the load capacitor not be discharged by the external spark gap. The inclusion of the HT diode between transformer and load alters this situation and the rundown of V_L in the absence of a discharge via the load resistor R_L is determined solely by the shunt loss in the load, which generally results in a slow rundown of V_L. Consequently a missed trigger pulse to the spark gap can result in a significant fraction of V_L being present on the load at the start of the next charge transfer. Firing a fully charged primary capacitor into the system with partly charged load capacitor results in a lower final load voltage than when firing into a fully discharged capacitor. There is thus no danger to equipment from a missed trigger pulse but it must be accepted that the voltage level of the subsequent cycle will be low and generally outside the permissible tolerance. In practice this would not seem to be a major problem because missed trigger pulses must in themselves be considered inadmissible and their consequences in subsequent cycles become irrelevant.

On balance it is considered that the advantages far outweigh the disadvantages. This is particularly the case for a power supply required for multi-shot ejection in which core recovery time if of overriding importance. Typical core recovery times of 10 - 20 milliseconds can be obtained with the present system, making multi-shot operation at 30 - 50 millisecond intervals a practical proposition as far as concerns the power supply.

6. Prototype power supply

A prototype power supply has been built to test out the foregoing theory. It was based on a 20 kVA 70 kV three winding transformer, the turns ratio being 55/17325/175 primary, secondary, tertiary, core cross-section 120 cm^2. The system was built for triple shot using three primary 13 mF banks each with its own SCR. The bias was run at 200 mA using either 0.66 kΩ or 1.1 kΩ as the tertiary damping resistor. The HT diode consisted of a stack of 15 Unitrode modules each rated 10 kV (see Fig. 8).

To date satisfactory triple shot charging of a 60 nF PFN has been accomplished at voltages up to 85 kV and 50 milli-second intervals. Triple shot charging at intervals of 35 milli-seconds has also been successful up to 70 kV - above this level difficulties occurred with the triggered spark gap for discharging the PFN.

An attempt has been made to predict the performance of this power supply from its equivalent circuit when charging 60 nF to 70 kV. Secondary voltage V_T and primary magnetising current I_M curves have been plotted (Figs. 9 and 10 respectively) for two values of damping resistor. These curves have been based on the following data.

Initial transformer flux density corresponding to - 200 mA tertiary bias	=	- 2600 gauss
Transformer flux density at end of charge transfer	=	4280 gauss
Change in magnetising current ΔI_M	=	1.74 A
$C_X + C_L$ = 60 nF		(1 nF + 59 nF)
C_0	=	13 mF
Magnetising inductance L_M	=	0.33 H
Equivalent resistance R_C	=	270 Ω

Stray capacitance, secondary C_S	=	560 pF
Leakage inductance $L_P + L_S'$	=	316 μH
Transformer resistance $R_P + R_S'$	=	40 mΩ
Filter resistance R_X	=	2.2 kΩ

The I_M curve (R_B = 1.1 kΩ) indicates a peak positive flux density of 8400 gauss and negative swing to - 4400 gauss when initially biased to - 2600 gauss. As the permissible $\hat{B}$ before reaching saturation is 16000 gauss, it should be possible with the present unit to charge 100 nF to 90 kV and remain within this limit. Increasing the tertiary bias current to 300 mA would enable this voltage to be raised to 100 kV.

The V_T curve shows charge transfer to be completed in 3.6 milliseconds. The negative swing of V_T (R_B = 1.1 kΩ) is approximately 50 % V_L, and crossover of the time axis occurs at 22 milliseconds after the SCR trigger. Oscillograms of V_T (R_B = 1.1 kΩ, Fig. 11) confirm the charge transfer time and indicate a negative swing of 43 % V_L with crossover time at 21 milliseconds. Unfortunately, these oscillograms had to be taken at a low voltage (V_L = 15 kV) because no fast high voltage divider was available. However, both the recovery time and the per unit negative swing should be independent of V_L provided that the elements of the equivalent circuit remain constant and that the magnetising current increases linearly with V_L. Both these conditions should be approximately satisfied up to $\hat{B}$ = 10000 gauss and hence the measurements at 15 kV can be considered representative of the situation at 70 kV. The time for commutation of the SCR (stage 2) has been calculated to be about 2.5 microseconds and this stage would therefore not be noticed on the oscillograms of Fig. 11. For all practical purposes in predicting power supply performance stage 2 may be ignored.

Fig. 12 shows oscillograms of transformer primary voltage, primary current, tertiary current and load voltage V_L when operating single shot at 70 kV into a 60 nF load. The V_L measurement is unfortunately distorted due to the poor frequency response of the HT divider - the true form of V_L is that of Fig. 11 recorded by Tektronix P6015 probe. A digital read-out of V_L voltage immediately prior to spark gap trigger showed a shot-shot variation of 0.2 kV.

Fig. 13 shows oscillograms of triple shot operation at 70 kV into 60 nF. The interval between shots is 50 milliseconds. Digital read-out of each flat top in turn confirmed that all three flat tops were of the same amplitude within 0.5 kV and that the cycle to cycle stability of the flat top of any one shot was better than 0.2 kV. It is therefore certain that the core recovery which has been theoretically predicted does in fact take place.

The cost of this prototype supply, excluding timing and digital voltage read-out, was about 17,000 SFr. inclusive of labour costs.

7. Conclusions

Operation of the prototype power supply for half a million shots has shown that a resonant power supply is a practical proposition for a multi-shot ejection system in which the time between shots is as small as 50 milliseconds. The performance of such a power supply can be closely predicted from its equivalent circuit and thus it should be possible to take maximum advantage of any given transformer core by designing for the largest possible flux swing. The inclusion of the HT diode in series with the power supply output brings with it greatly improved operating flexibility and a less onerous voltage specification for the pulse forming network. The continuous bias running in the transformer tertiary is simple and effective. The form of the core recovery is to some extent controllable by adjustment of the damping resistance.

The results from the prototype are sufficiently encouraging to justify further expenditure for the construction of a six-shot system to be used as a laboratory supply for the testing of components of the new full aperture kicker system.

8. Acknowledgements

The authors would like to express their recognition of the valuable suggestions made by H. S. Simpson during the design and construction of the prototype power supply and for his excellent contribution during the gathering and evaluating of the experimental results. The authors would also like to thank Messrs. Brückner and Cupérus for the interesting technical discussions at the outset of this development.

9. References

(1) "A resonant charging pulsed high voltage power supply"
A. Brückner, J.F. Labeye. SI/Int./MAE 68-6

(2) "A fast charging power supply for the delay lines of the kicker magnet pulsers"
J. Cupérus. PS/FES/Int. 68-5

Distribution: open

10. List of figures

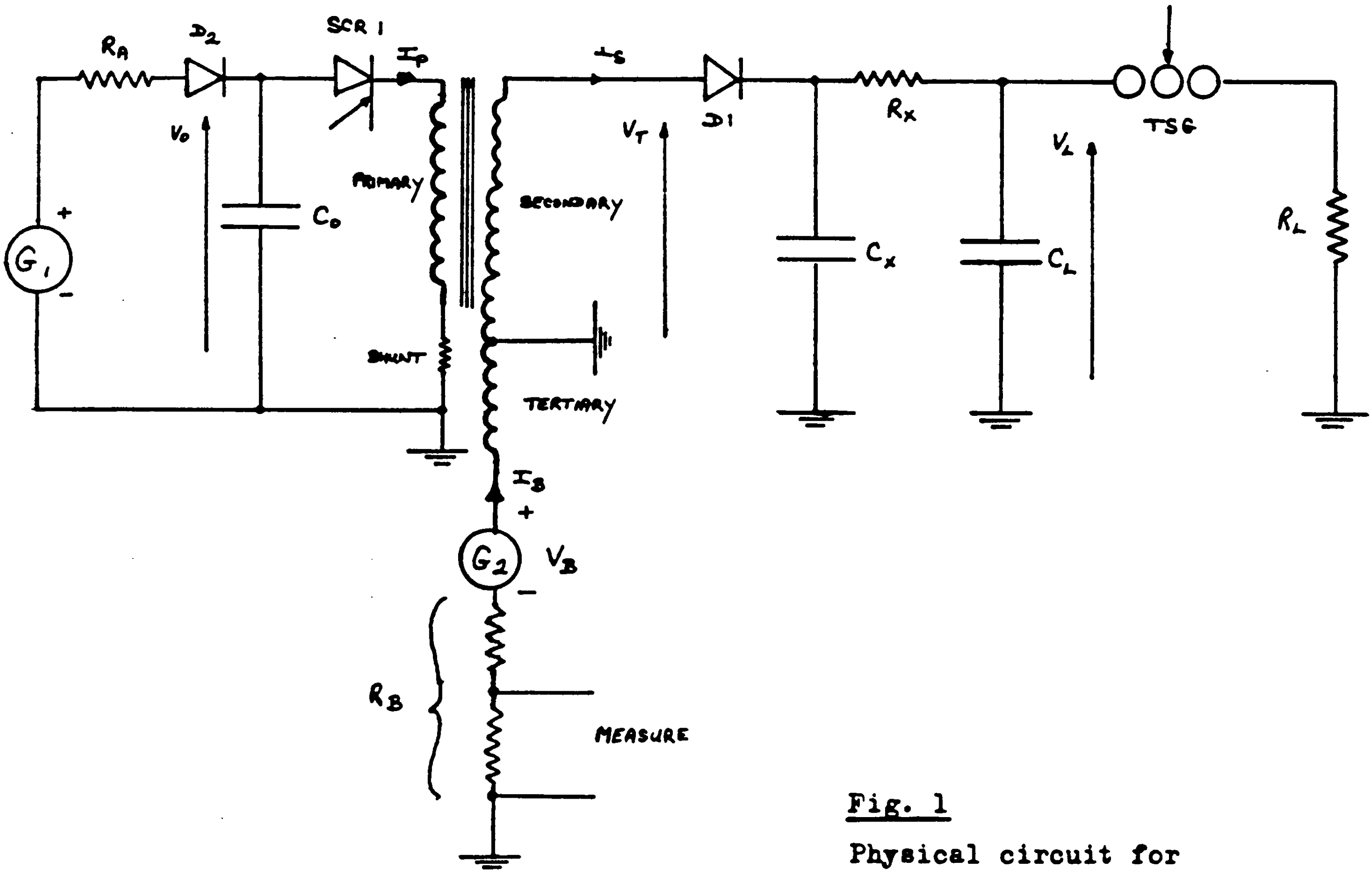

Fig. 1

Physical circuit for single shot operation

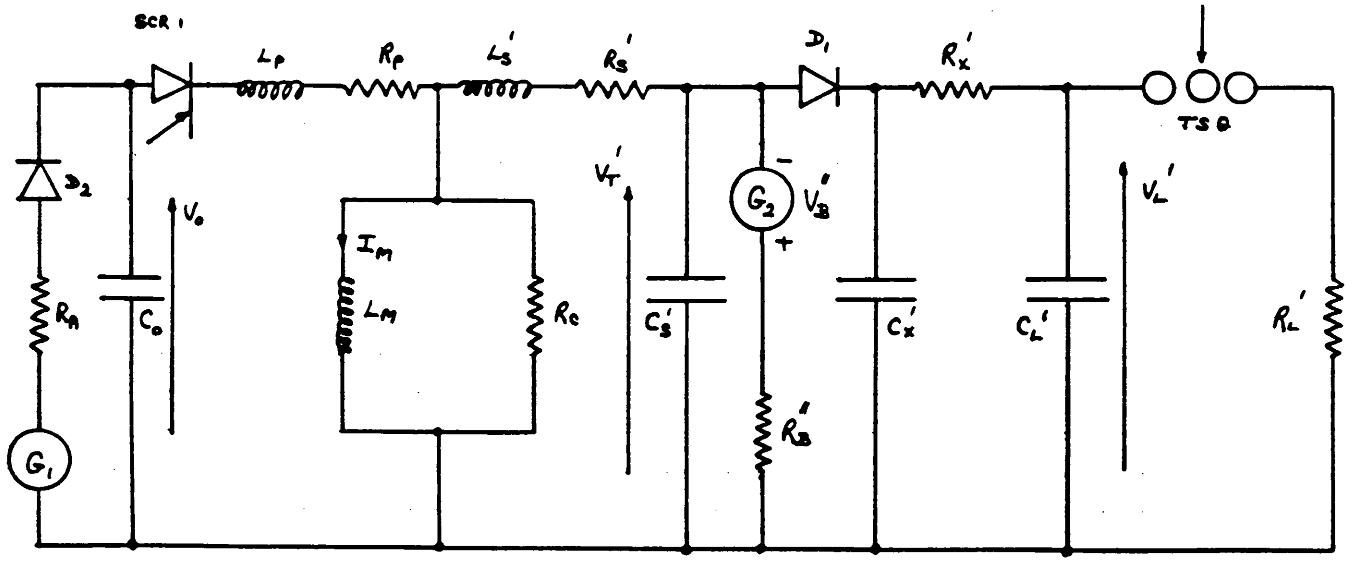

Fig. 2

Full equivalent circuit of Fig. 1, referred to primary

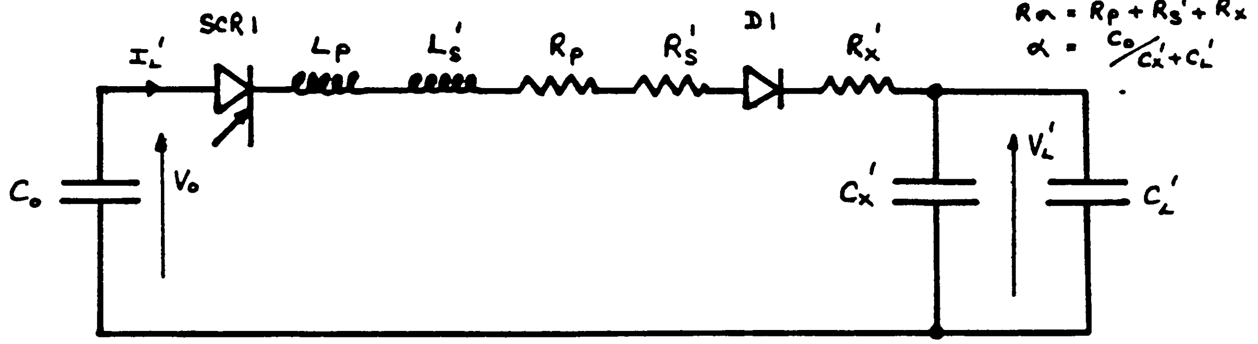

Fig. 3 Simplified equivalent circuit during Stage 1 (charge transfer)

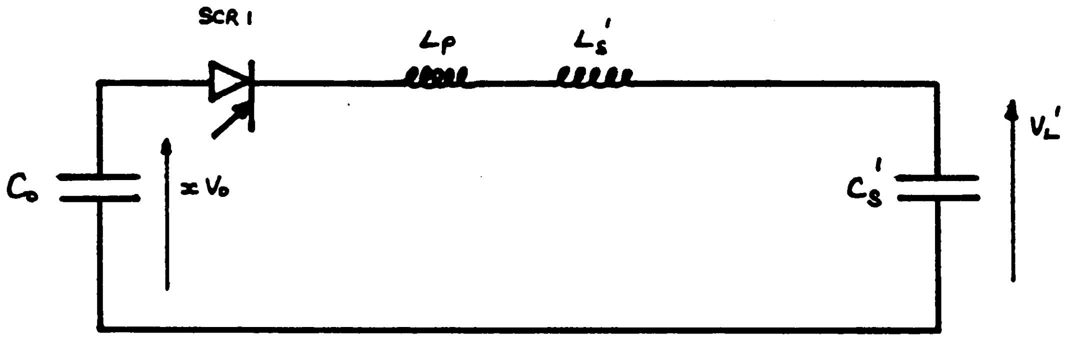

Fig. 4 Simplified equivalent circuit during Stage 2 (disconnection of C_o)

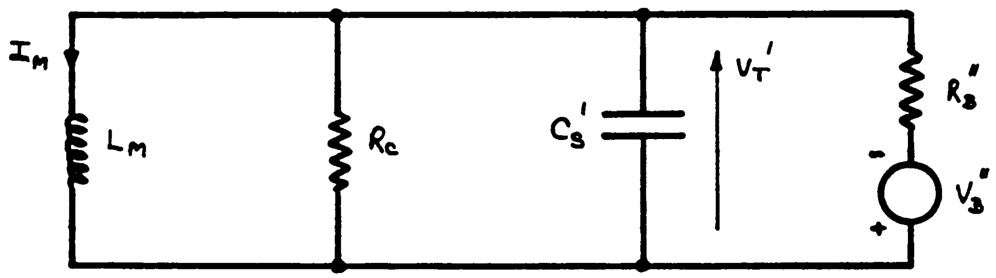

Fig. 5 Simplified equivalent circuit during Stage 3 (core recovery with $V_T < V_L$)

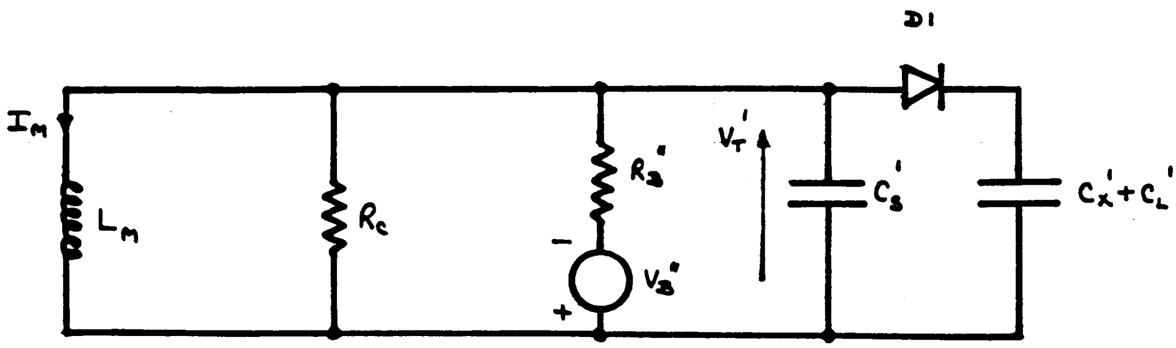

Fig. 6 Simplified equivalent circuit during Stage 4 (core recovery with $V_T \geq V_L$)

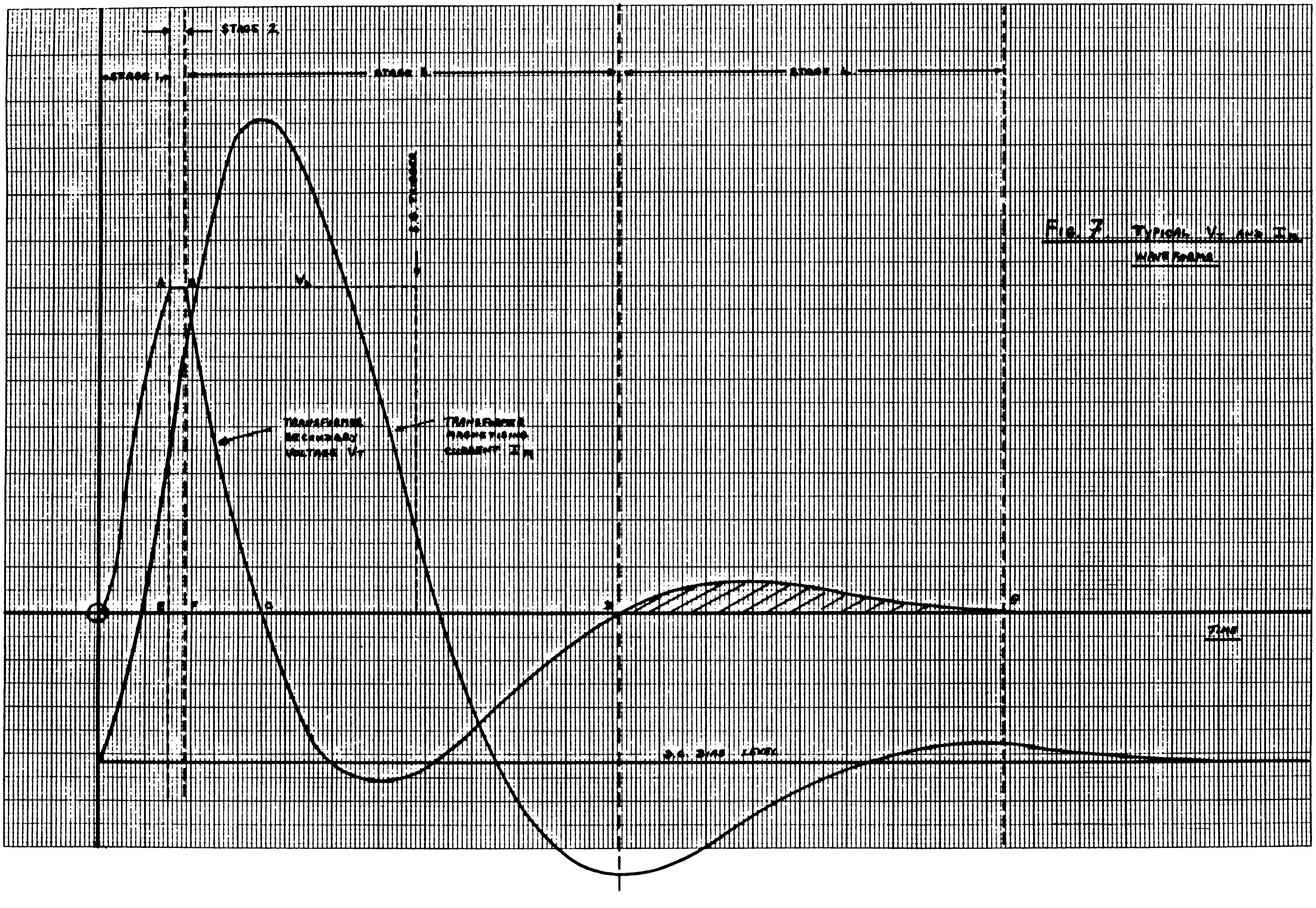

Fig. 7 Typical V_T and I_M Waveforms

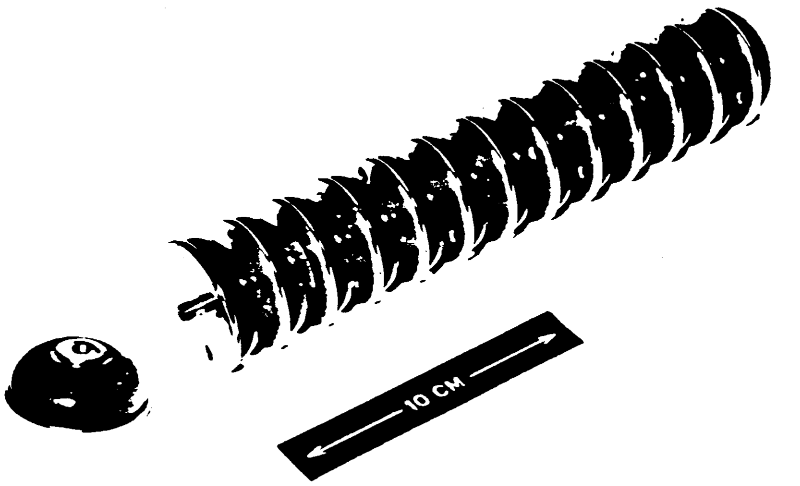

Fig. 8 HT Diode Assembly (Unitrode) for 140 kV

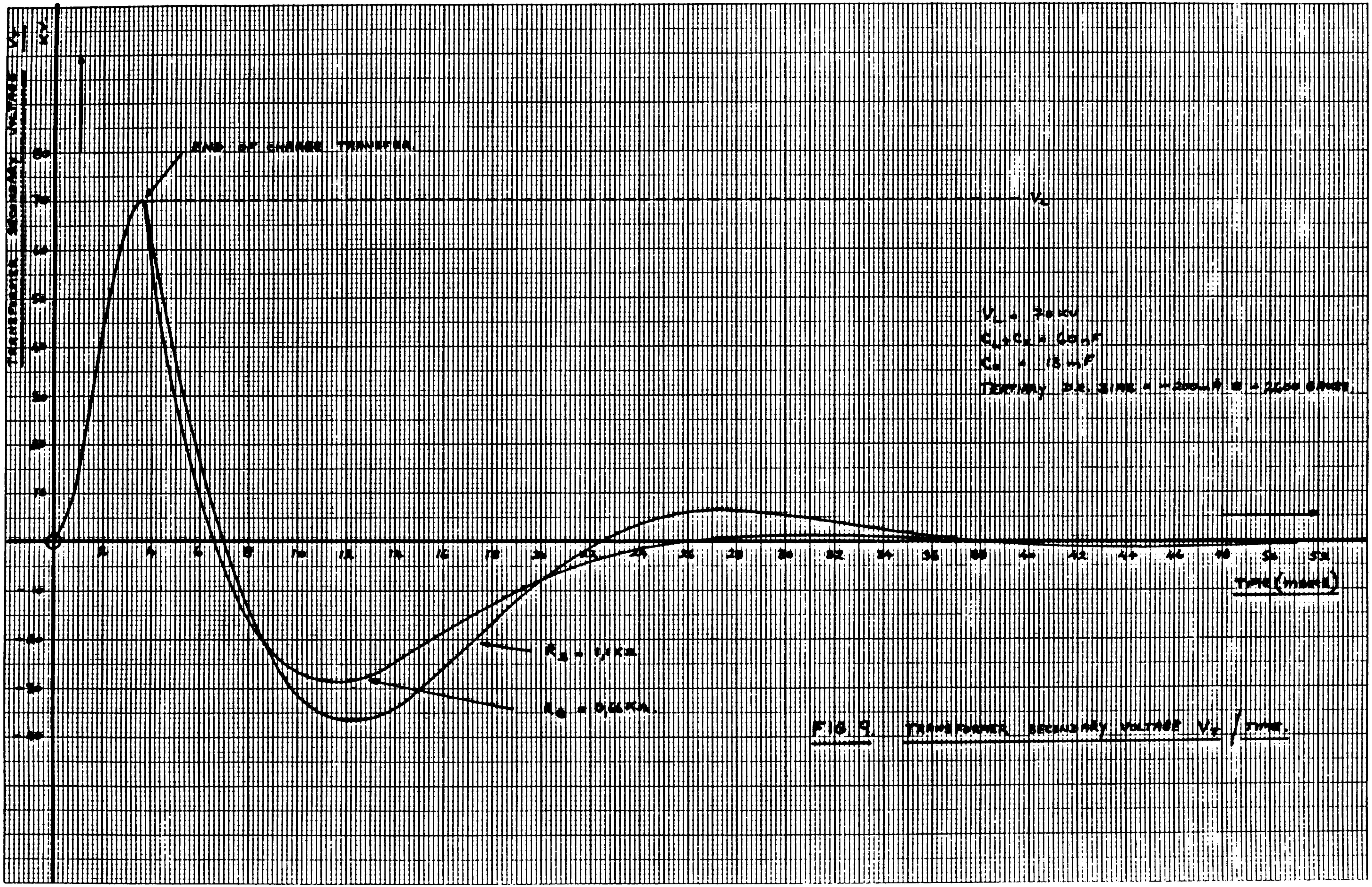

FIG 9. TRANSFORMER SECONDARY VOLTAGE V_T / TIME.

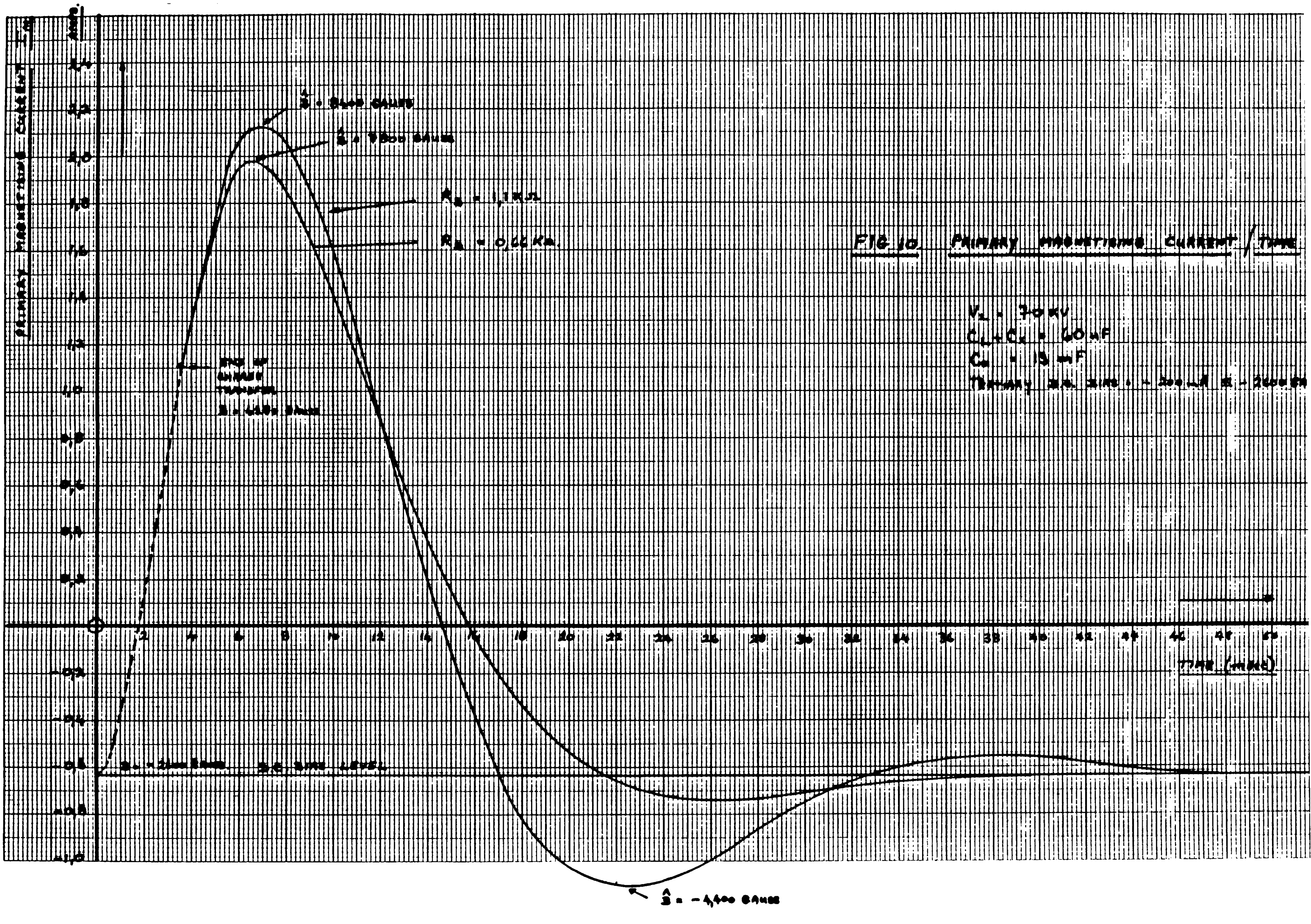

FIG 10. PRIMARY MAGNETISING CURRENT / TIME

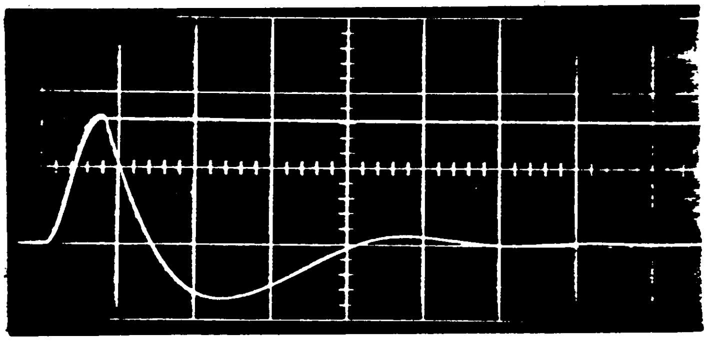

S.G. Trigger = SCR Trigger + 69 msecs.

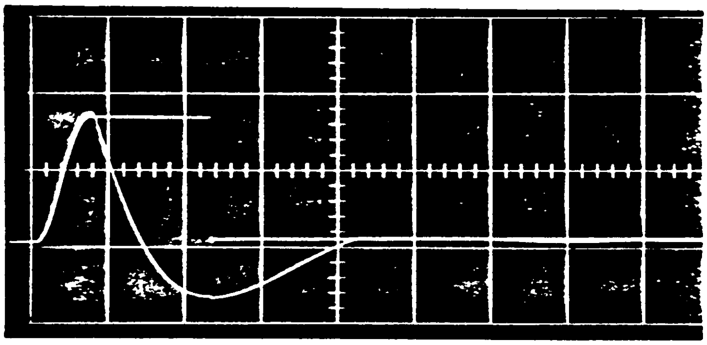

S.G. Trigger = SCR Trigger + 11 msecs.

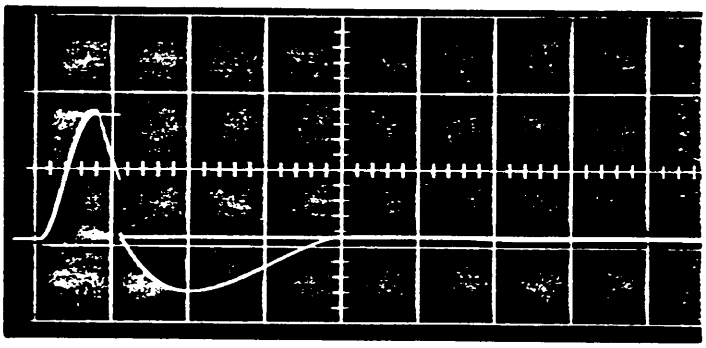

S.G. Trigger = SCR Trigger + 5 msecs.

10 kV/cm (Tektronix P6015 probe)

5 millisecs/cm

Primary voltage 48.2 Volts

Load 60 nF

Tertiary bias - 200 mA

R_B 1.1 kOhms

Fig. 11 Load Voltage V_L and Transformer Secondary Voltage V_T as function of V_L flat top

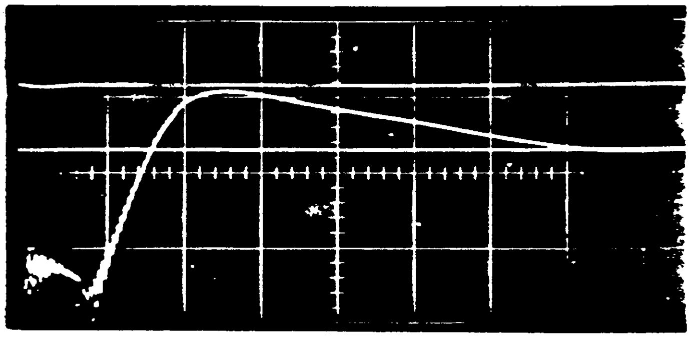

0 mA	228 mA/cm (Tektronix P6008 probe)
- 200 mA	5 msecs/cm

SG Trigger = SCR Trigger + 10 msecs.
V_L = 70 kV
Load = 60 nF
Tertiary bias - 200 mA
R_B = 1.1 kOhms

Fig. 12a Current in tertiary resistor R_B

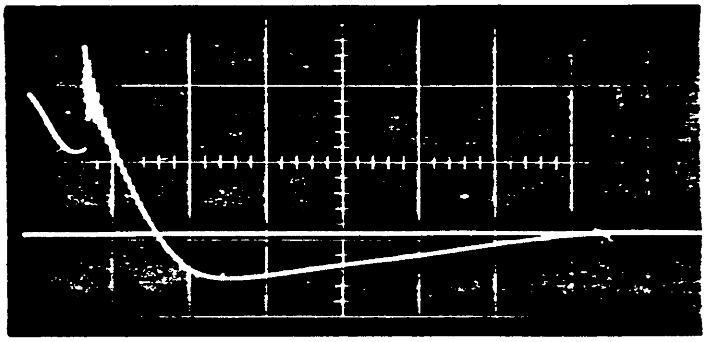

100 V/cm (Tektronix P6008 probe)
5 msecs/cm
SG Trigger = SCR Trigger + 10 msecs.
V_L = 70 kV
Load = 60 nF
Tertiary bias - 200 mA
R_B = 1.1 kOhms

Fig. 12b Transformer primary voltage

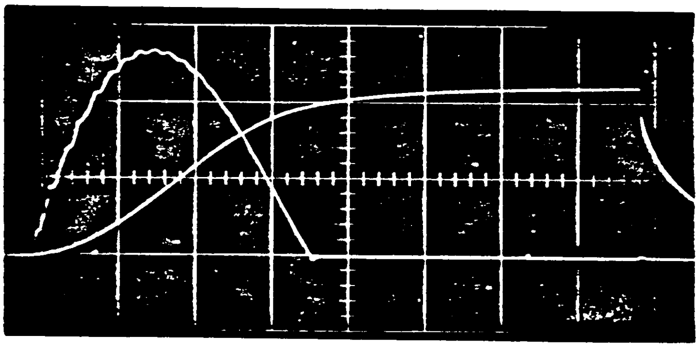

Primary current 200 A/cm
Load voltage 31 kV/cm (Haefely divider)
1 msec/cm
SG Trigger = SCR Trigger + 8 msecs.
V_L = 70 kV
Load = 60 nF
Tertiary bias - 200 mA
R_B = 1.1 kOhms

Fig. 12c Primary current I_P and load voltage V_L

Fig. 12 Single shot charging of 60 nF load to 70 kV

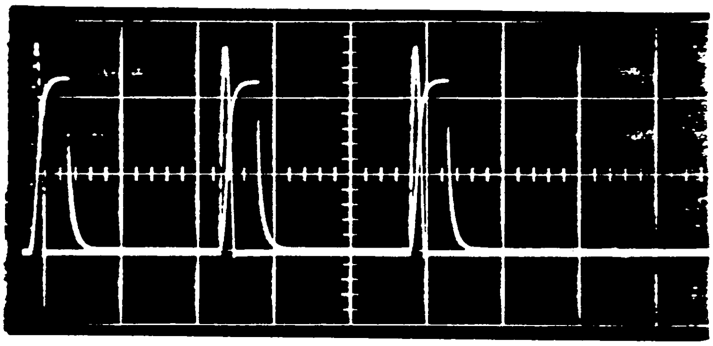

Primary current 200 amps/cm

Load voltage 31 kV/cm

20 msecs/cm

SG Trigger = SCR Trigger + 10 msecs.

Primary current 500 amps/cm

Load voltage 62 kV/cm

20 msecs/cm

SG Trigger = SCR Trigger + 10 msecs.

Photo used for report for IEEE Pulse Modulator Symposium 1973.

V_L = 70 kV

Load = 60 nF

Tertiary bias - 200 mA

Primary capacitor 3 x 13 mF

R_B = 1.1 kOhms

Fig. 13 **Triple shot operation, primary current I_p and load voltage V_L.**